Numerical Investigation on Transition Mechanisms in a Laminar Separation Bubble with Increasing Reynolds Number

A. Samson[1], Karthik Naicker[2], S. S. Diwan[1]

[1]Department of Aerospace Engineering, IISc, Bangalore, India.

[2]Associate Engineer, Caterpillar India Pvt. LTD.

Motivation

- Aerodynamics performance of aerofoils operating at low-Reynolds numbers is of immense importance as it is marked by low lift and high drag due to flow separation [Muller and DeLaurier 2003]
- Under these conditions, flow transition to turbulence occurs due to the concomitant effects of boundary layer streaks (observed in FST induced transitional boundary layers) and the coherent structures from the separated boundary layer due inviscid instability [Istvan and Yarusevych 2018, McAuliffe and Yaras 2010, Zaki et al. 2010, Blazer and Fasel 2016 and Lardeau et al. 2012].

- The problem has received huge interest for its practical applications.
  - → flow through compressor passage
  - → flow over wings of unmanned aerial vehicles
  - → small-to-medium size wind turbine blades
  - → Low-pressure Turbine (LPT) blades

Motivation

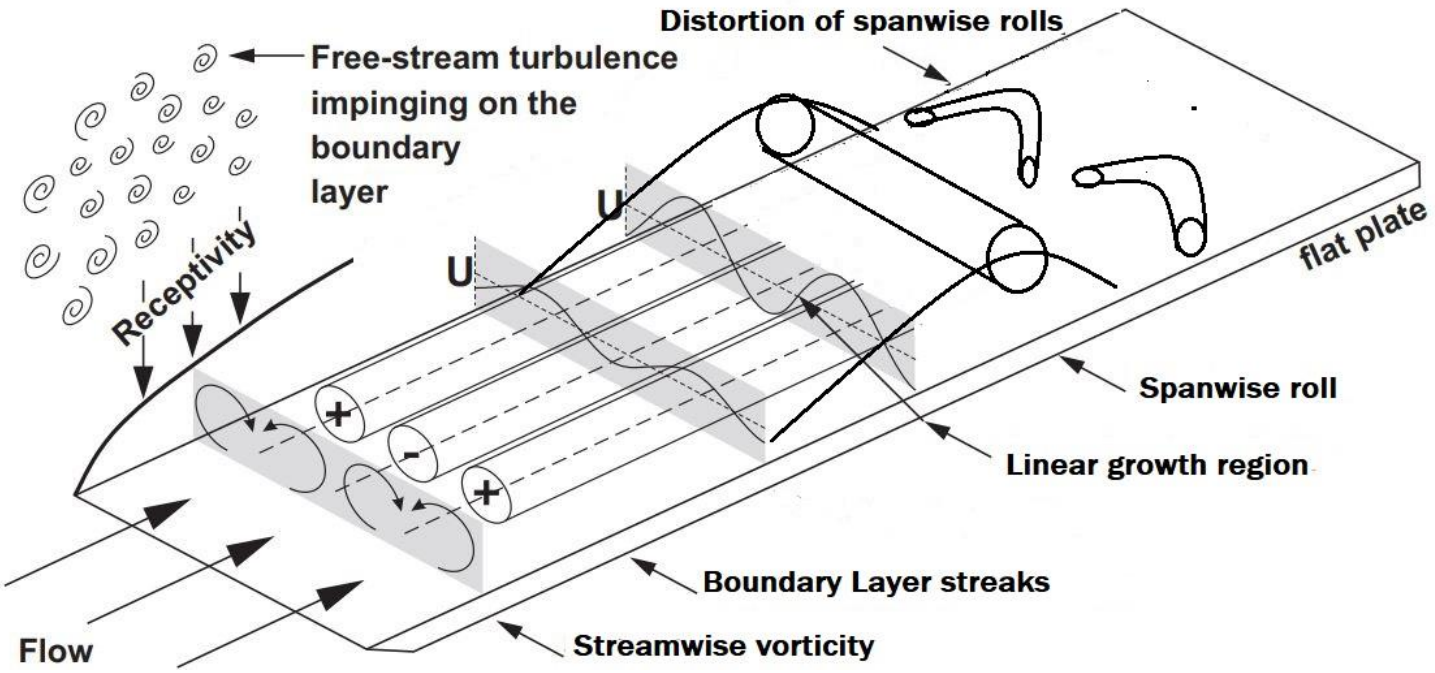

Schematic representing the transition mechanism, where boundary layer streaks and spanwise rolls for separated shear layer interact

Motivation

- **Such a scenario has been studied through experiments and numerical simulations on Flat plate and compressor blades**

→ Experiments by Haggmark (2000) on a flat plate, Istavan and Yarusevych (2018) on an aerofoil.

→ DNS of Zaki et al (2010) on compressor blade and Lardeau et al. (2012) flat plate and compressor blade .

→ Numerical Simulations of McAullife and Yaras (2010) and Brinkerhoff and Yaras (2011) works of Fasel and group (2016,2019) on flat plate with adverse pressure gradient.

→ Inferences: Low FST - K-H instability; High FST – K-H instability is bypassed; 3-D structures due to spanwise distortion

Objective and Outstanding Questions

- **Understanding the change in mechanism of transition as the boundary layer character changes from separated to an attached under the influence of adverse pressure gradient for varying Re at inlet FST of 10.23% that decays to 0.3%.**

1. **Can turbulent spots be formed as a result of interaction between streamwise streaks and separated boundary layer**
2. **If turbulent spots form can we detect them by examining the time variation of the velocity**
3. **Can we ascribe/attribute the route to transition is through formation of turbulent spots if the intermittency agrees with that of universal intermittency**

Solver

- DNS code developed by Dr. Saurabh Patwardhan, IISc
- Quantities have been non-dimensionalised
  - δ_{in}^{*}– Displacement thickness at inlet
  - U_{ref} - incoming free-stream velocity
- Code solves the incompressible NS equations using the fractional step method
- Integration in time is carried out with 3rd order Runge - Kutta
- A rectangular Cartesian domain , with staggered grid approach
  - Central difference scheme, second order accurate in space
  - Domain divided into 2400*300*240

Grid and Boundary Conditions

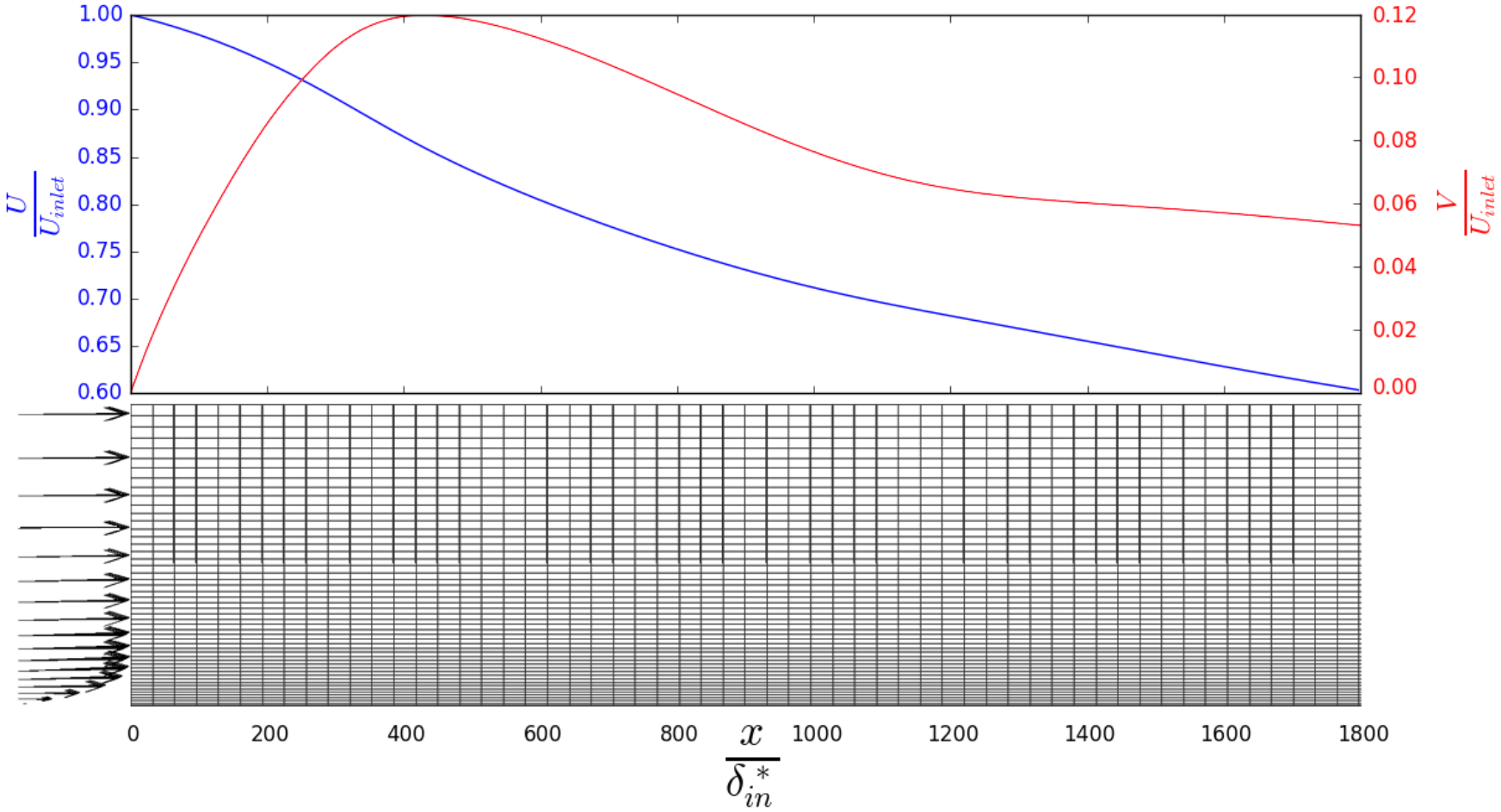

Computational domain with grid and boundary conditions

Grid resolution in wall units comparison with literature

Case	$\Delta x+$	$\Delta y+$ at $y+ = 9$	$\Delta z+$	N($y+<9$)
Alam and Sandham (2000), case 3DF-B	14.26	0.87	6.3	17
Jones et al. (2008), case 3DF	3.36	>1	6.49	69
Marxen and Henningson (2011), case reso1	6.53	0.94	11.06	10
Balzer and Fasel (2016)	5.6	0.9	6.15	18
Present Work	**2.87**	**0.6**	**3.07**	**20**
Hosseinverdi and Fasel (2019) (with FST)	1.58	0.44	2.71	25

Change in Transition mechanism in APG Separated Boundary Layers

Mean Flow details illustrating change in flow character

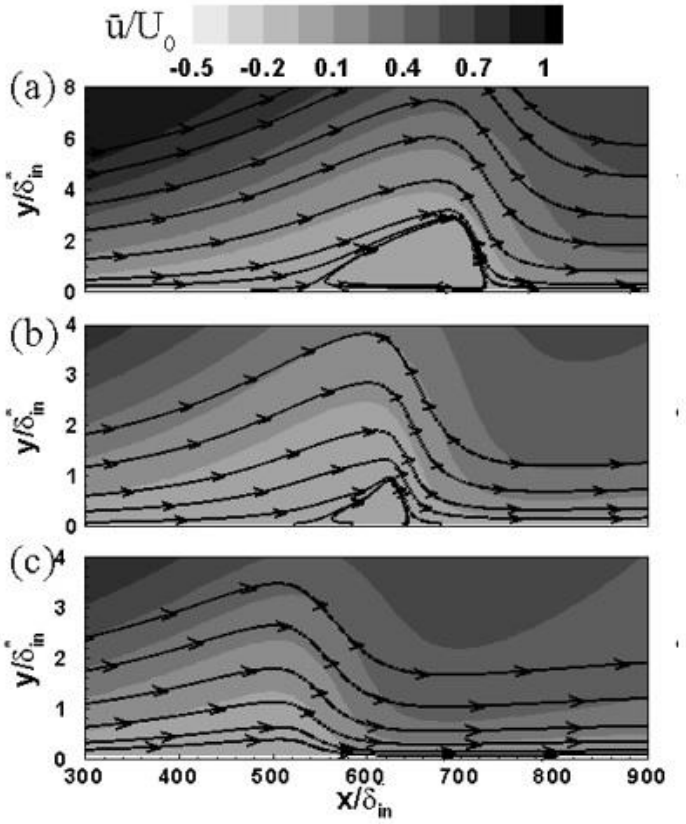

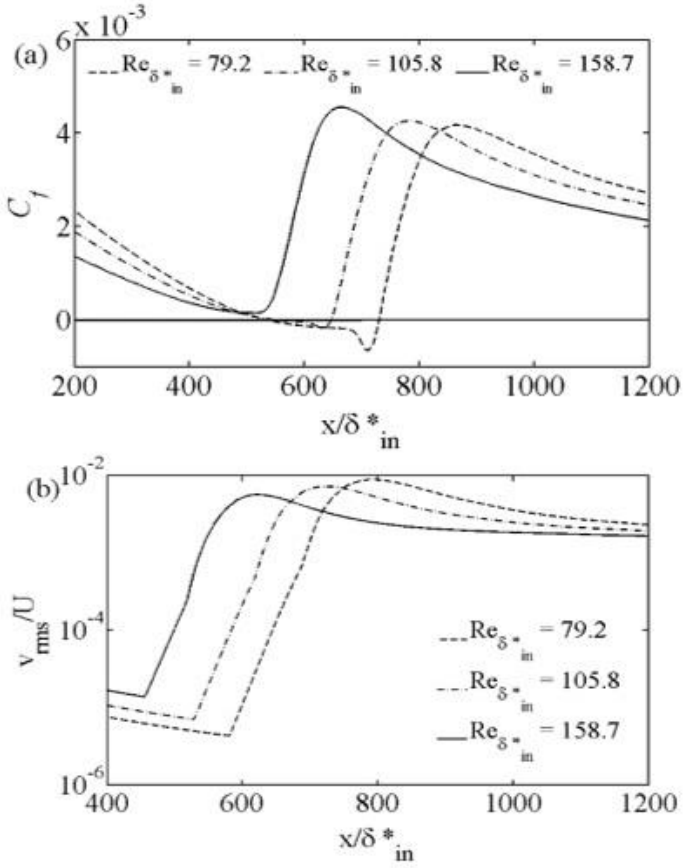

Left Pane: change in flow character with increasing $Re_{\delta_{in}^*}$, $Re_{\delta_{in}^*}$ = 79.2 (top); $Re_{\delta_{in}^*}$ = 105.8 (middle) and $Re_{\delta_{in}^*}$ = 158.7 (bottom).

Right Pane: (a) Variation of skin friction coefficient for varying $Re_{\delta_{in}^*}$ and (b) Effects of $Re_{\delta_{in}^*}$ variation on the growth of wall-normal velocity fluctuations.

Change in Transition mechanism in APG Separated Boundary Layers

Mean Flow details illustrating change in flow character

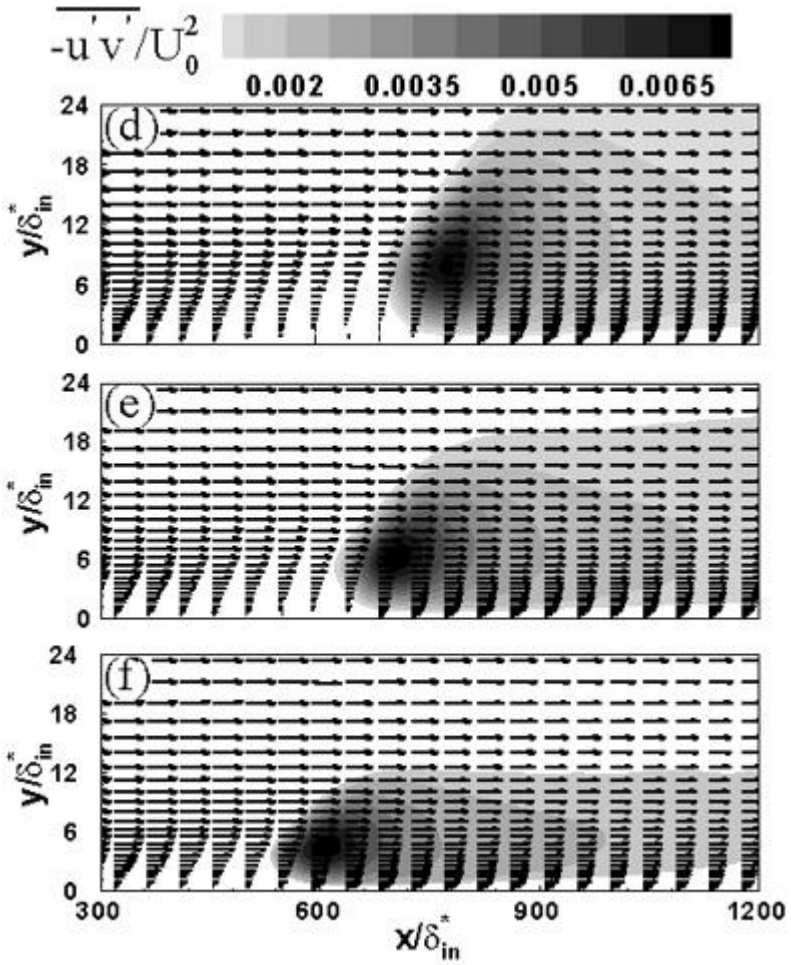

Change in flow character with increasing $Re_{\delta^*_{in}}$, $Re_{\delta^*_{in}}$ = 79.2 (top); 105.8 (middle) and 158.7 (bottom).

- Transition, in separated boundary layer is associated with velocity fluctuations being amplified resulting in increase of Reynolds stress.
- The onset of transition is marked as the location where the value of normalised Reynolds stress is 0.001 [Ol et al. 2005].
- For separated flow, boundary layer transition is initiated in the separated shear layer with increasing values of stress in the downstream of the maximum height of the bubble, with maximum values of stress in the vicinity of reattachment away from wall indicating enhanced outer layer activity owing to breakdown of large-scale structures

Change in Transition mechanism in APG Separated Boundary Layers

Evolution of streamwise and wall-normal velocity fluctuations and flow visualizations

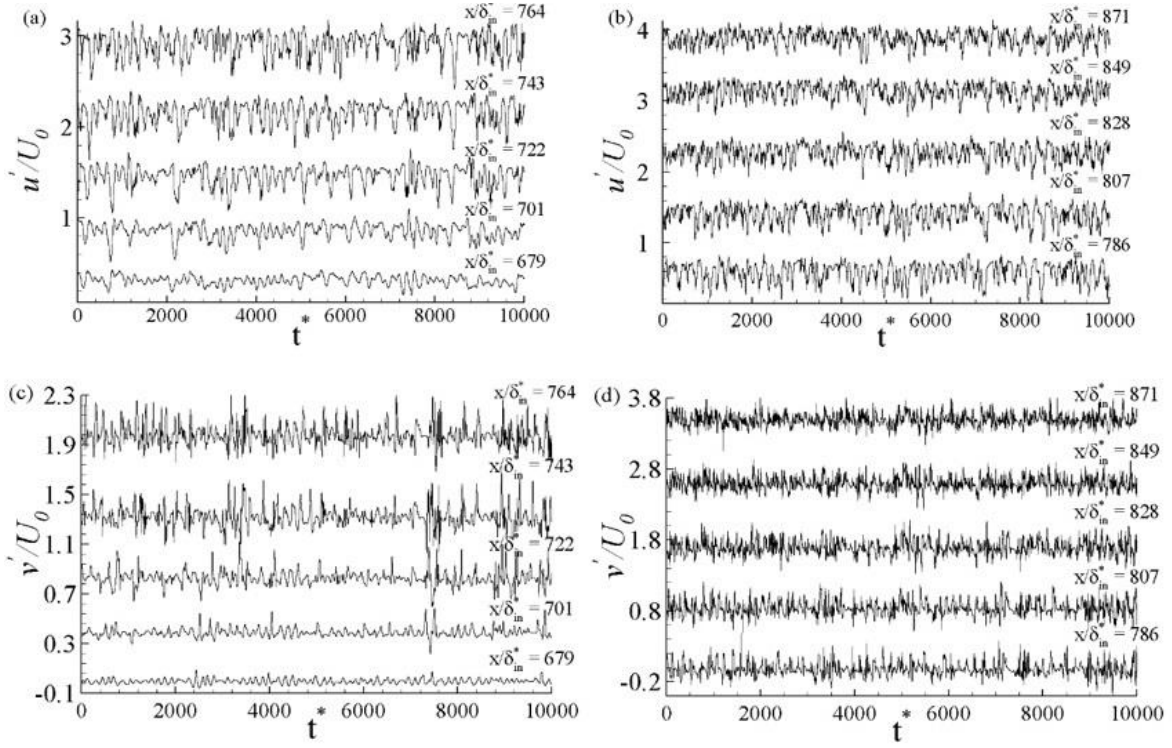

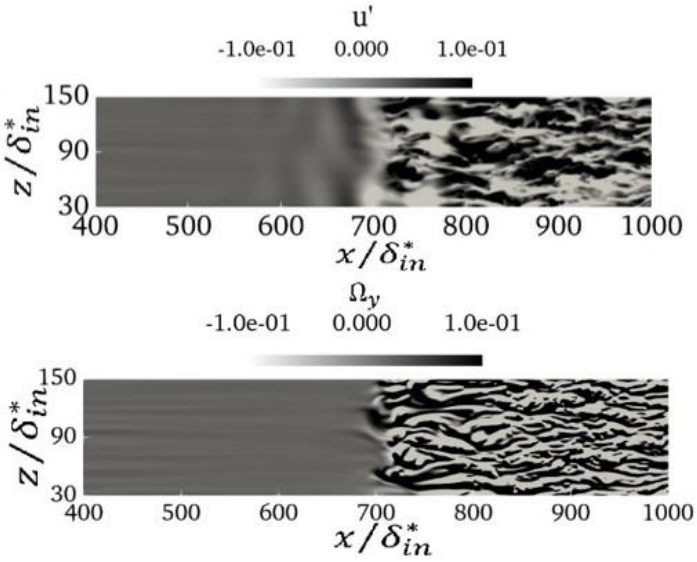

Evolution of streamwise and wall-normal velocity fluctuations for $Re_{\delta^*_{in}}$ = 79.2: (a) and (b) streamwise velocity and © and (d) wall-normal

Flow visualizations illustrating breakdown of spanwise rolls leading to three-dimensional motions

Change in Transition mechanism in APG Separated Boundary Layers

Evolution of streamwise and wall-normal velocity fluctuations and flow visualizations

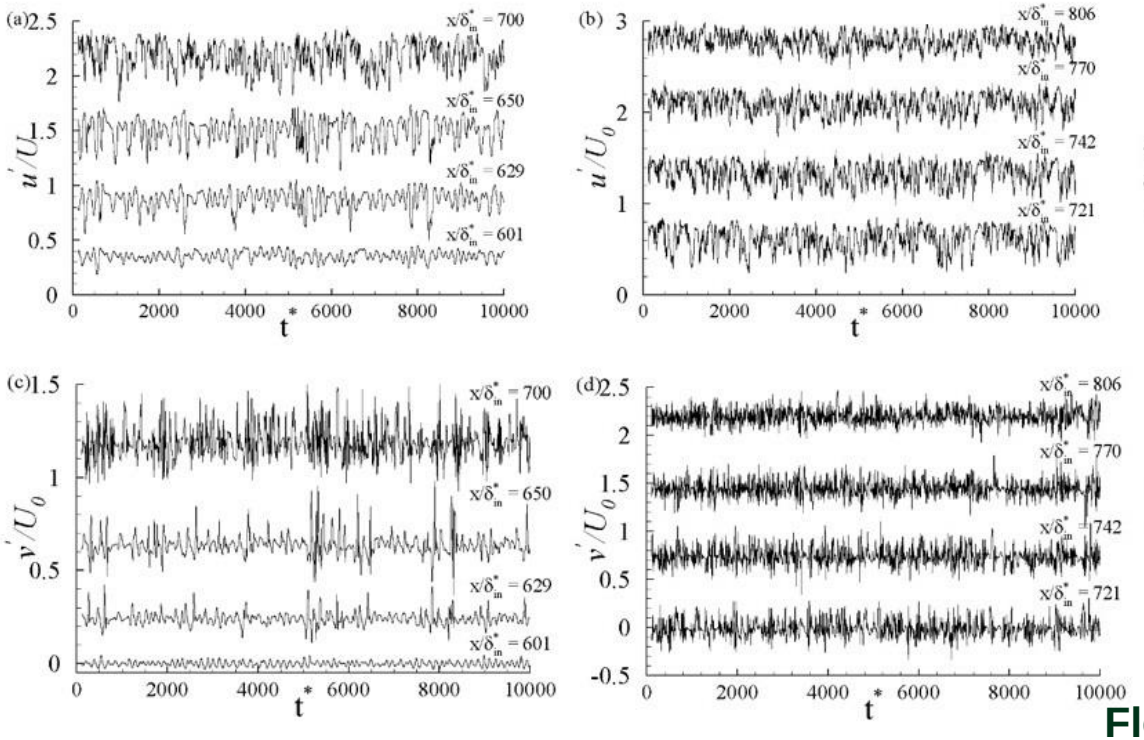

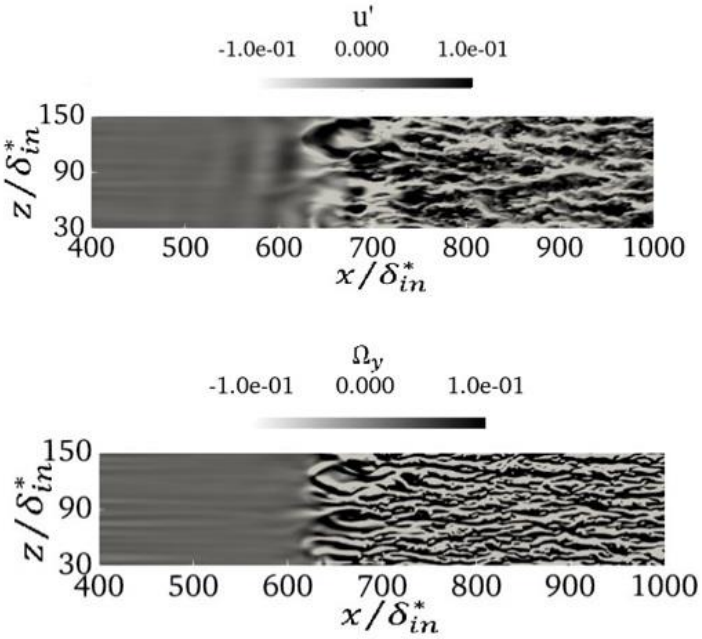

Evolution of streamwise and wall-normal velocity fluctuations for $Re_{\delta^*_{in}}$ = 105.8 : (a) and (b) streamwise velocity and © and (d) wall-normal

Flow visualizations illustrating interactions of streaks and spanwise rolls leading to distortions of spanwise rolls resulting in formations of turbulent spots

Change in Transition mechanism in APG Separated Boundary Layers

Evolution of streamwise and wall-normal velocity fluctuations and flow visualizations

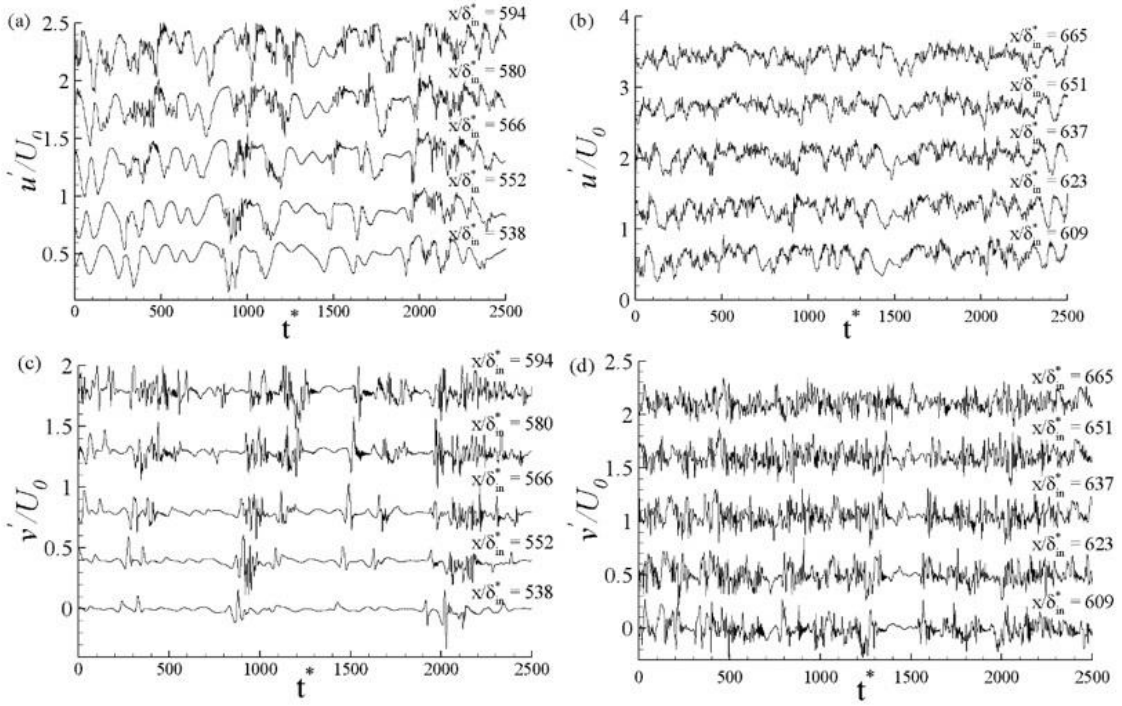

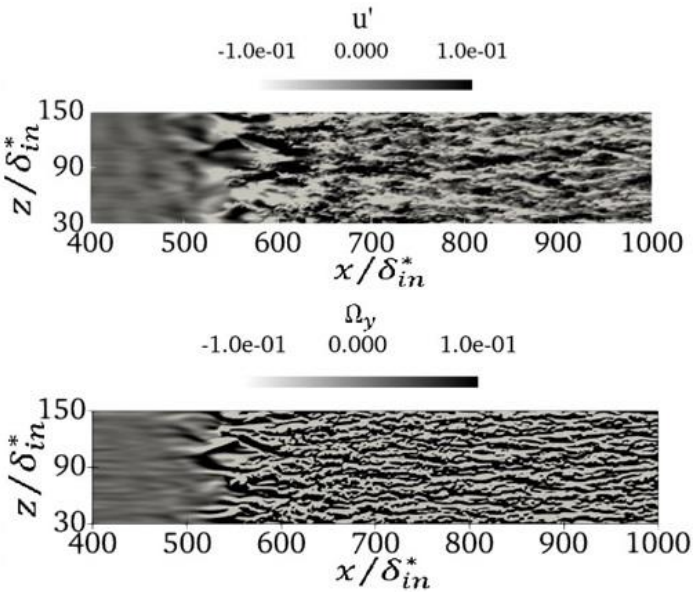

Evolution of streamwise and wall-normal velocity fluctuations for $Re_{\delta^*_{in}}$ = 158.7 : (a) and (b) streamwise velocity and © and (d) wall-normal

Flow visualizations illustrating breakdown of streaks leading to formation of turbulent spots.

Change in Transition mechanism in APG Separated Boundary Layers

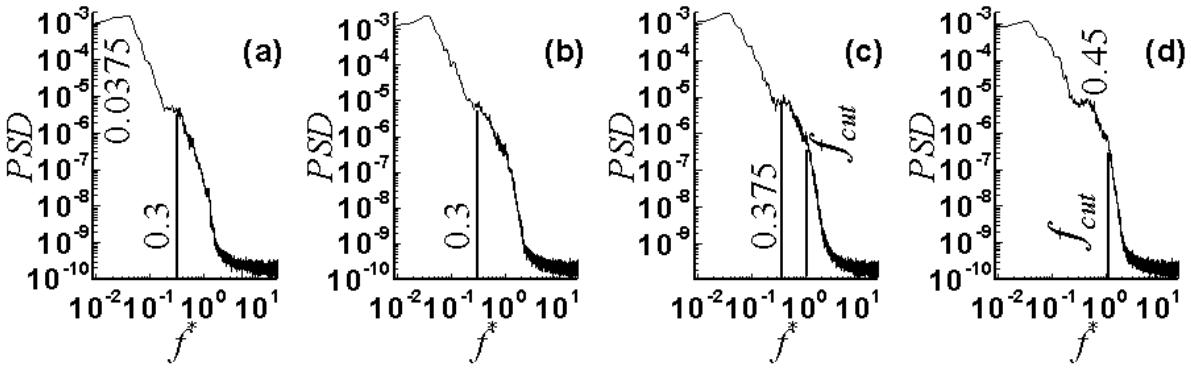

Spectra for $Re_{\delta^*_{in}}$ = 79.2; (a) to (d) X/δ^*_{in} = 722;764;807 and 849

- **Kh = 1.25; indicates inviscid instability**

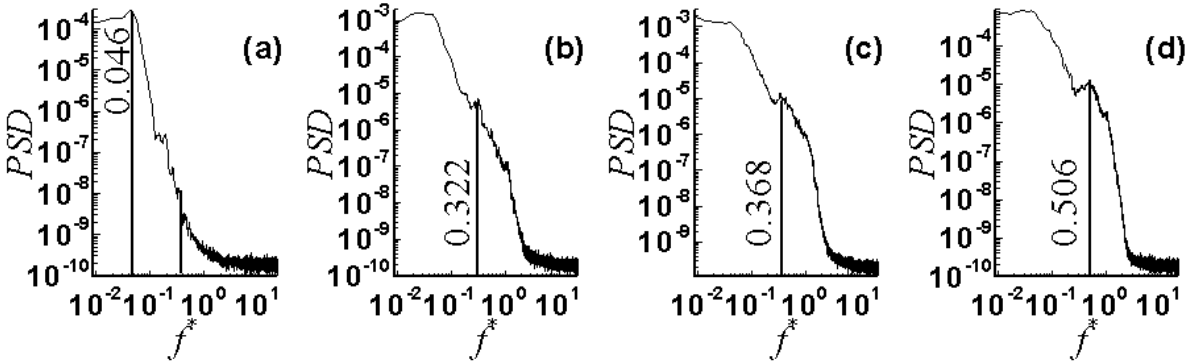

Spectra for $Re_{\delta^*_{in}}$ = 105.8; (a) to (d) X/δ^*_{in} = 601;650;700 and 770

- **Kh = 1.08; indicates inviscid instability**

Change in Transition mechanism in APG Separated Boundary Layers

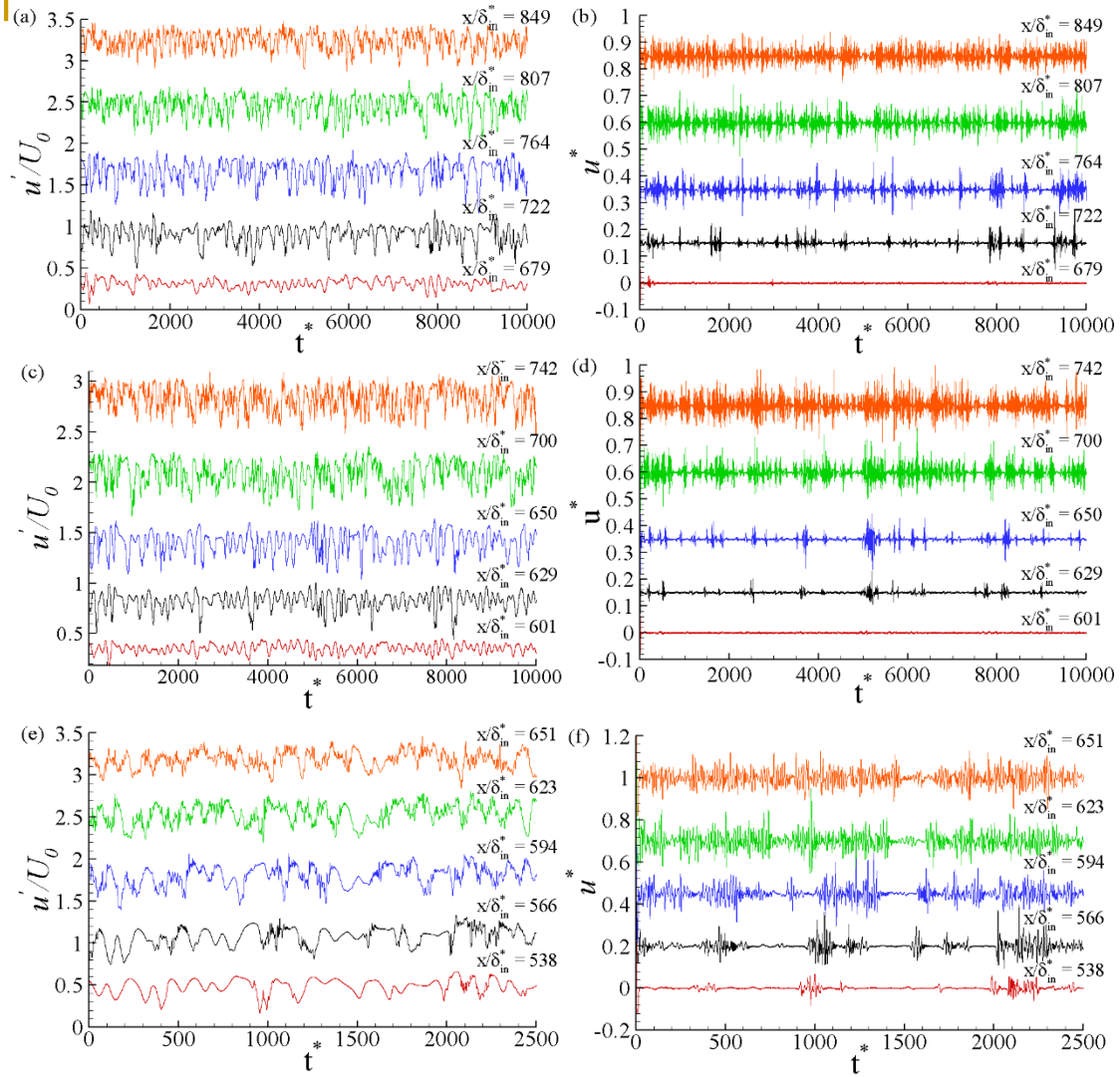

- **Emmons' [1951] description of turbulent spots: localised high frequency regions has been appropriately contested after high pass filtering of the streamwise velocity for all $Re_{\delta^*_{in}}$**
- **Fast Fourier Transform (FFT) of the velocity signals has been carried out to choose a cut-off beyond the most amplified frequency**
- **In a separated flow, low-frequency components in the signal are the most amplified frequencies. Therefore, the choice of the cut-off is a multiple of the most amplified frequency beyond the actual value**

Comparison of raw and filtered time traces illustrating turbulence spot as $Re_{\delta^*_{in}}$ increases.

Change in Transition mechanism in APG Separated Boundary Layers

Interactions of streaks and separated boundary layer

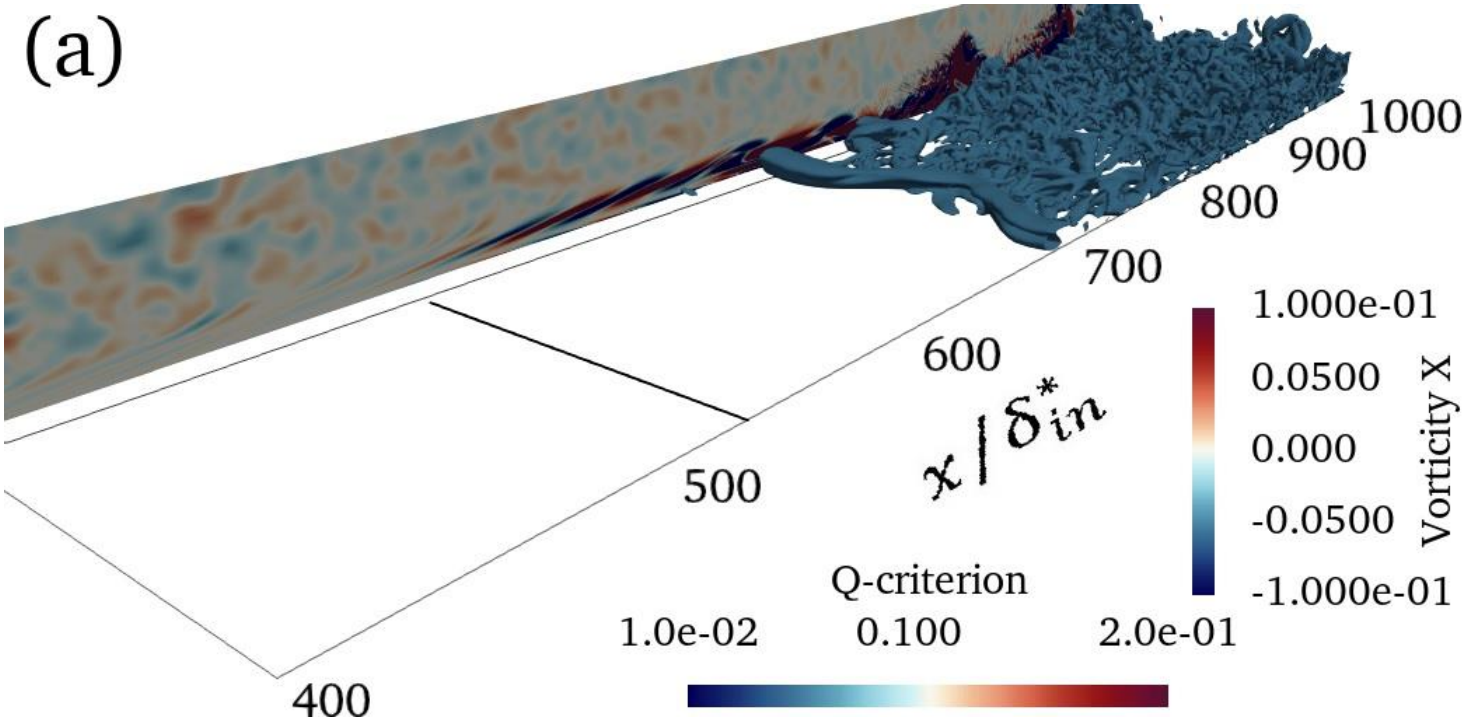

Contours of instantaneous streamwise vorticity showing breakdown the separated shear layer.

Change in Transition mechanism in APG Separated Boundary Layers

Interactions of streaks and separated boundary layer

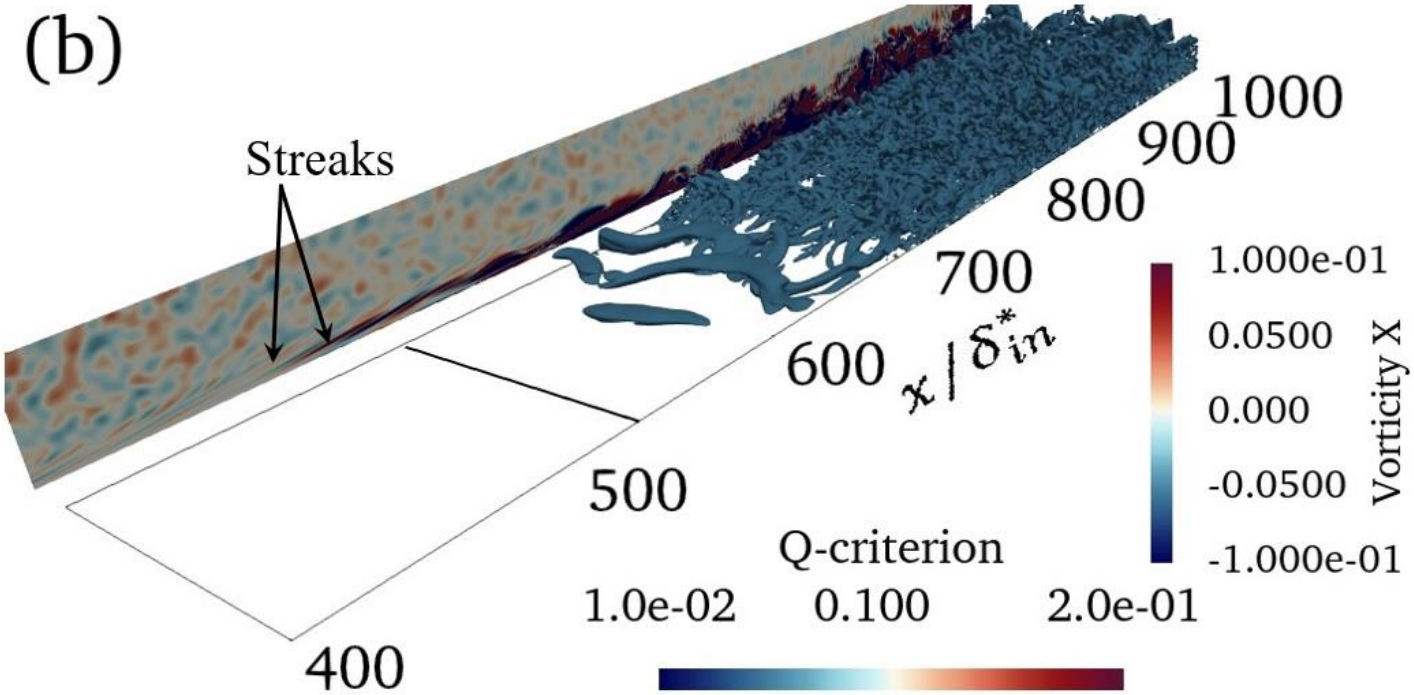

Contours of instantaneous streamwise vorticity showing formation of boundary layer streaks and its interaction with the separated shear layer.

Change in Transition mechanism in APG Separated Boundary Layers

Interactions of streaks and separated boundary layer

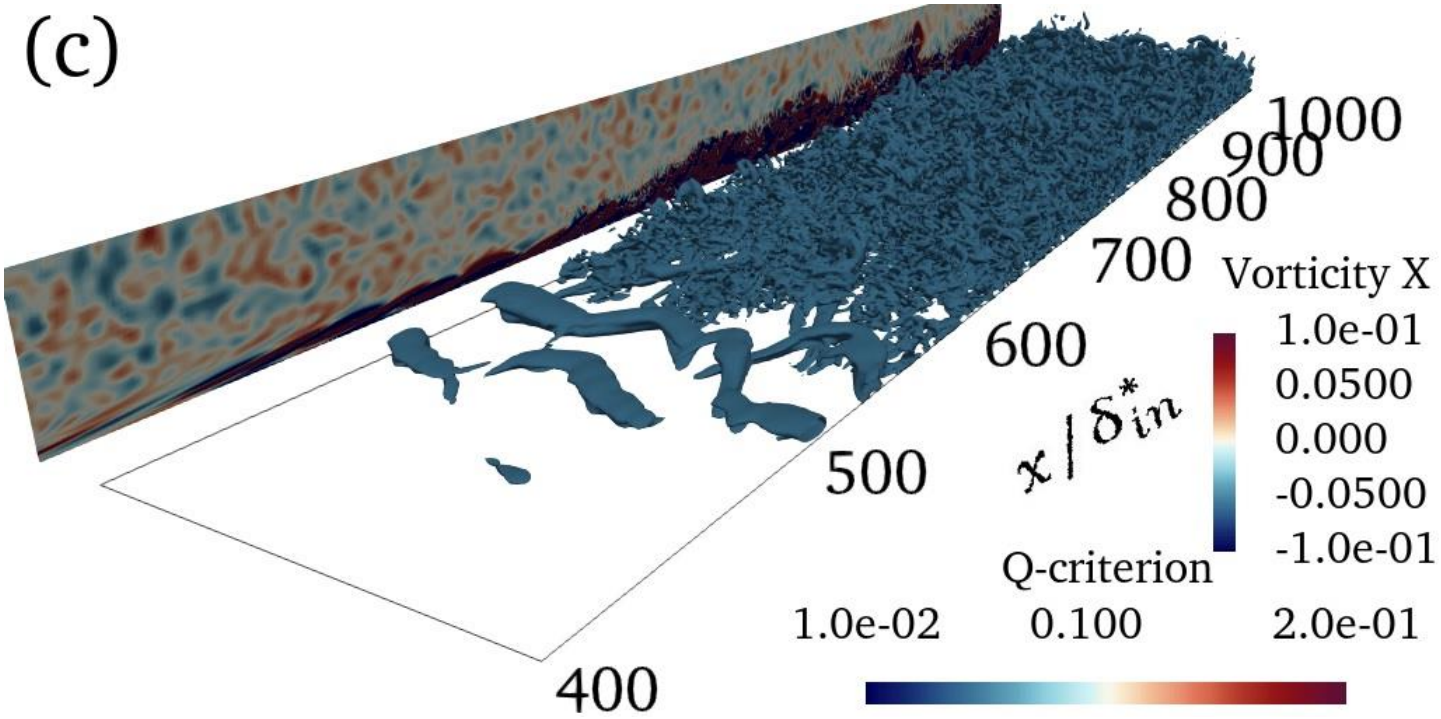

Contours of instantaneous streamwise vorticity showing formation of boundary layer streaks and breaking down small-scale structures.

Change in Transition mechanism in APG Separated Boundary Layers

Intermittency variation

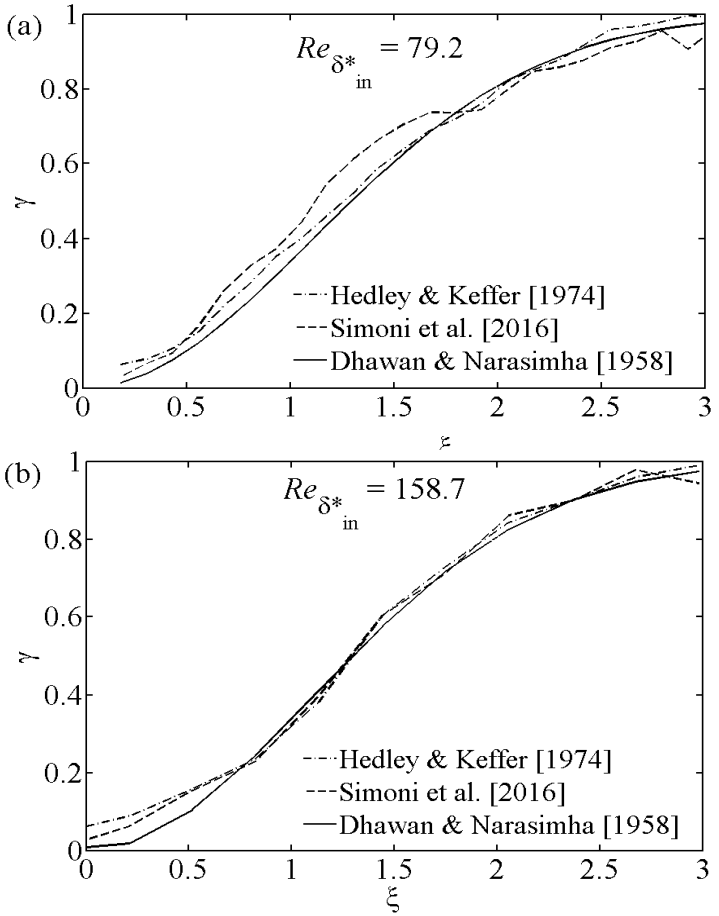

- **In the past, some studies [Samson and Sarkar 2016 and Simoni et al. 2018] have inferred evidences of spot formation in the transition of separated boundary layer for varying Re and Tu.**
- **Although time evolution of velocity along with instantaneous flow visualizations do not reveal existence of turbulence spots the plausible reason for intermittency variation comparing well with universal intermittency of Dhawan and Narasimha [1957] may be attributed to amplification of disturbances and breakdown of spanwise structures.**

intermittency comparison with universal intermittency curve of Dhawan and Narasimha [1958], (a) for Large bubble case and (b) for attached flow case.

Noteworthy Interpretations

- At low $Re_{\delta_{in}^*}$ the boundary layer transition occurs due to inviscid instability and turbulent spots are not evident in time traces and in flow visualizations.

- However, intermittency variation agrees well with that of universal intermittency, The plausible reason for intermittency variation comparing well with universal intermittency is attributed to amplification of disturbances and breakdown of spanwise structures in the downstream of reattachment, which manifest as high frequency disturbances

- At $Re_{\delta_{in}^*}$ = 105.8, in the downstream of maximum height of the bubble, time traces show localized disturbances akin to turbulent spots that begin to grow and becomes maximum in the vicinity of reattachment. Flow visualization reveal interactions between boundary layer streaks and spanwise structures resulting in deterioration of dominant coherent structures and breakdown to turbulent spots.

- At high $Re_{\delta_{in}^*}$, time traces reveal a sinusoidal oscillation owing to formation of streaks and predominantly show regions of localised disturbances, which grows in time and persist until region of maximum skin friction coefficient (C_f).

Thank You

Additional Slides

$$\frac{\partial \boldsymbol{u_i}}{\partial \boldsymbol{x_i}} = 0 \ (1)$$

$$\frac{\boldsymbol{\partial u_i}}{\boldsymbol{\partial t}} + \boldsymbol{u_j}\frac{\boldsymbol{\partial u_i}}{\boldsymbol{\partial x_j}} = -\frac{\boldsymbol{\partial P}}{\boldsymbol{\partial x_i}} + \frac{\boldsymbol{1}}{\boldsymbol{Re}}\frac{\boldsymbol{\partial^2 u_i}}{\boldsymbol{\partial x_j \partial x_j}} \quad (\boldsymbol{2})$$

$$\frac{\partial u_i}{\partial t} = \underbrace{-\frac{\partial u_i u_j}{\partial x_j}}_{A} + \underbrace{\frac{1}{Re}\frac{\partial^2 u_i}{\partial x_j \partial x_j}}_{D} \underbrace{-\frac{\partial P}{\partial x_i}}_{P} \quad (3)$$

$$\frac{\partial u_i^*}{\partial t} = -\frac{\partial u_i u_j}{\partial x_j} + \frac{1}{Re}\frac{\partial^2 u_i}{\partial x_j \partial x_j} \quad (4)$$

$$\frac{\partial u_i}{\partial t} = \frac{\partial u_i^*}{\partial t} - \frac{\partial P}{\partial x_i} \quad (5)$$

$$\frac{\partial}{\partial t}\left(\frac{\partial u_i^*}{\partial x_i}\right) = \frac{\partial^2 P}{\partial x_j \partial x_j} \quad (6)$$

Based on this, we can summarise the process a below -

Step 1 - Using equation 4, calculate intermediate velocity field u_i^* using the known velocity field u_i at time step t.

Step 2 - Using the u_i^* calculated in the above step, solve Poisson equation 6 for the pressure field P.

Step 3 - Using the intermediate velocity field u_i^* and the pressure field determined above, use equation 5 to determine the velocity field u_i at next time step t + t.

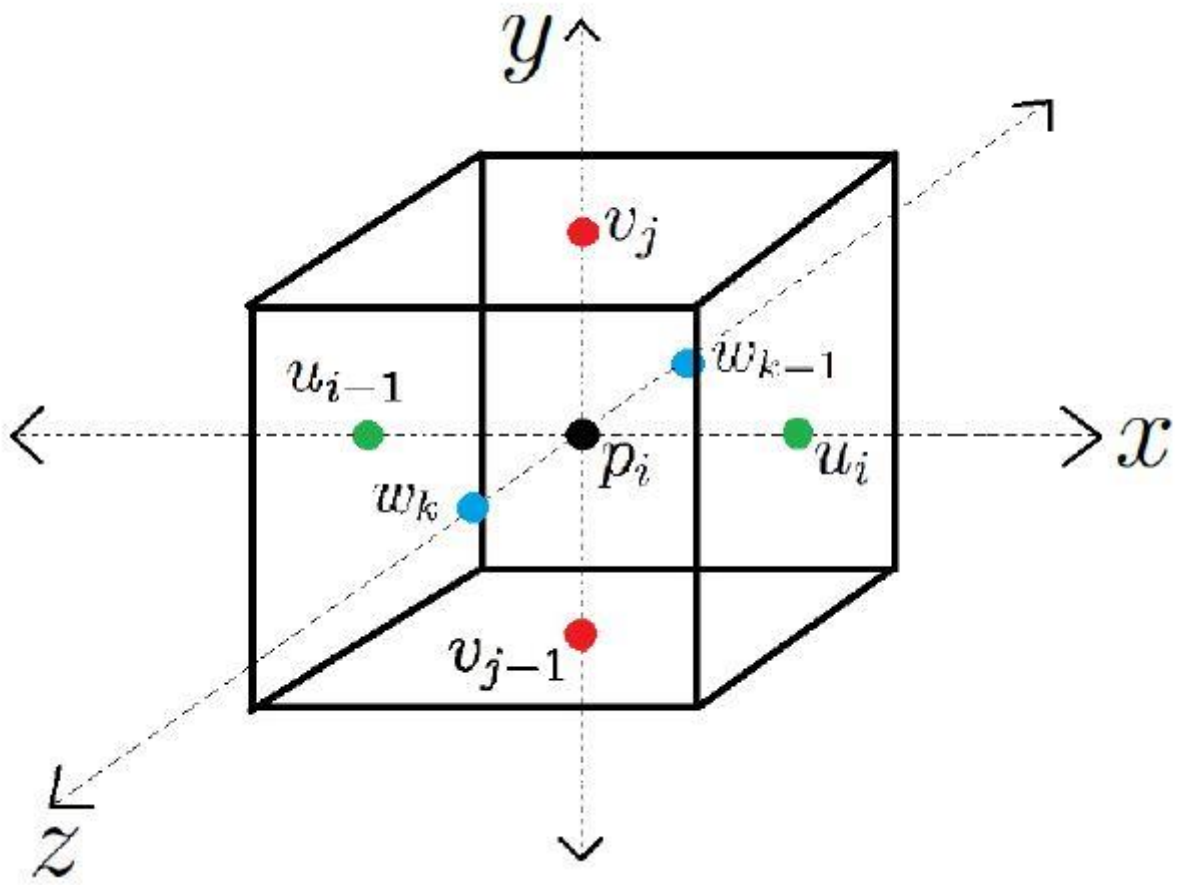
y
v_j
u_{i-1}
w_{k-1}
p_i
u_i
x
w_k
v_{j-1}
z

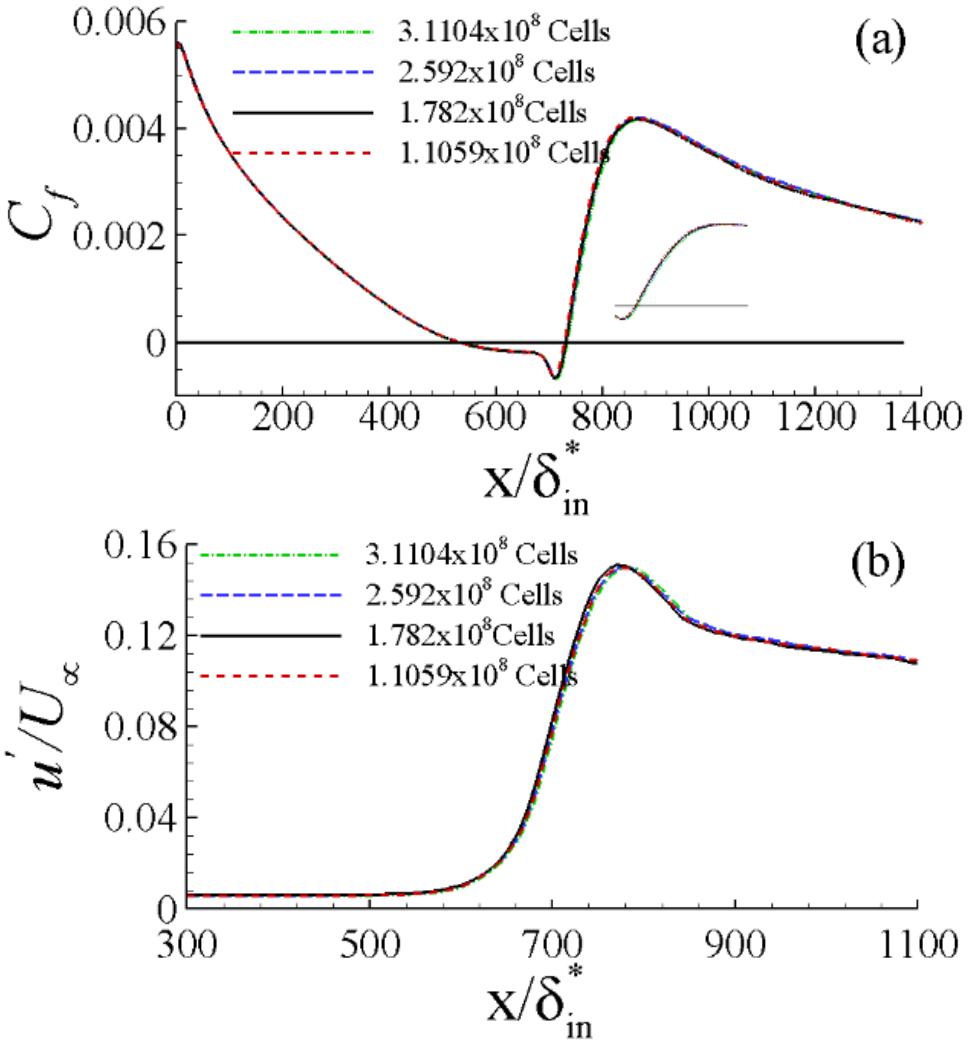
(a)
3.1104x10^8 Cells
2.592x10^8 Cells
1.782x10^8Cells
1.1059x10^8 Cells
C_f
0.006
0.004
0.002
0
0
200
400
600
800
1000
1200
1400
x/δ^*_{in}
(b)
3.1104x10^8 Cells
2.592x10^8 Cells
1.782x10^8Cells
1.1059x10^8 Cells
u'/U_∞
0.16
0.12
0.08
0.04
0
300
500
700
900
1100
x/δ^*_{in}

Wavelet-based intermittency detection technique (Simoni et al. (2016))

2 ways to determine intermittency –

- Based on times series obtained by hotwire
- Based on PIV data using wavelet method

Methodology –

- PIV data acquired
- Wavelet analysis of data
- Based on data, probability density function is defined
- Intermittency function obtained based on PDF

Continuous wavelet transform of a generic 1D signal

$$w(x,s) = s^{-1/2} \int f(x') \psi^* \left(\frac{x' - x}{s} \right) dx'$$

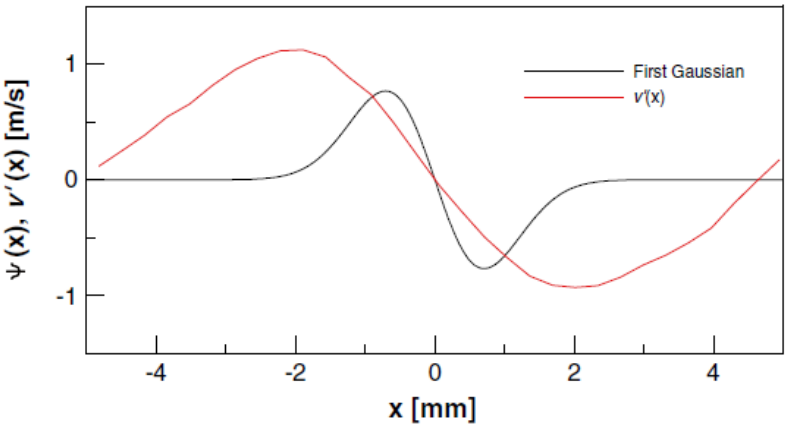

Figure - Comparison of fluctuating velocity signal and First Gaussian Wavelet (Simoni et al (2016))

Wavelet-based intermittency detection technique (Simoni et al. (2016))

- Calculating wavelet energy

$$E(x,y,s) = \frac{\sqrt{\left[w(s)_{1,2}w^*(s)_{1,2}\right]\left[w(s)_{2,1}w^*(s)_{2,1}\right]}}{s}$$

- Filtering the data

$$E(x,y,s) > \left[\bar{E}(s) + q\sigma\{E(x,y,s)\}\right]$$

- Selecting scale

$$e(s) = \int\int E(x,y,s)\mathrm{d}x\mathrm{d}y$$

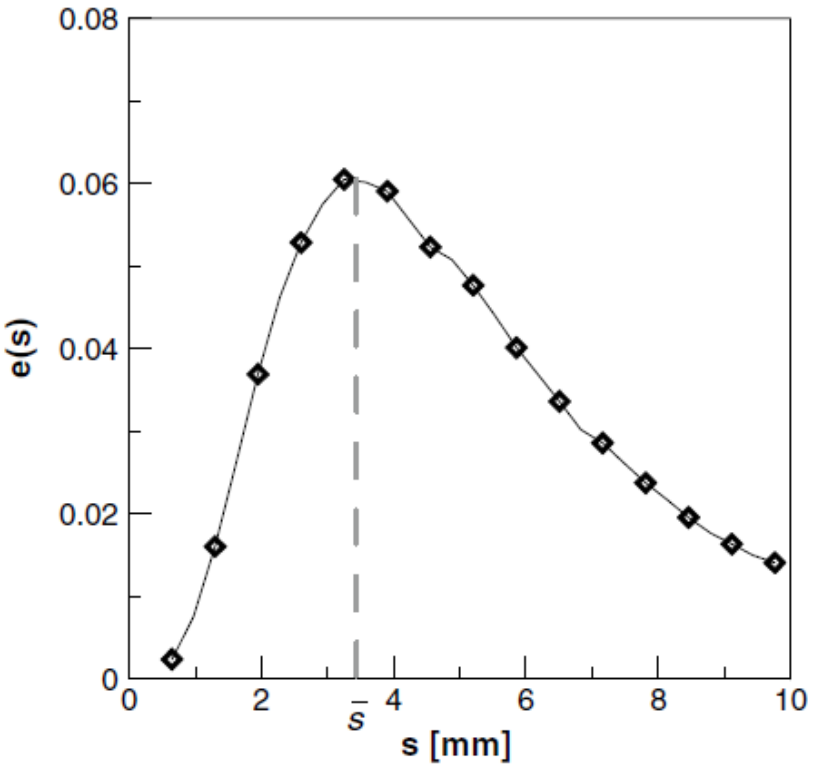

First Gaussian wavelet energy spectrum of data, Simoni et al (2016)

Wavelet-based intermittency detection technique (Simoni et al. (2016))

- Streamwise Variation

$$\tilde{e}(x,s) = \Sigma_i \int E_i(x,y,s)\mathrm{d}y$$

- Define counter function (N),
- use counter function to define PDF

$$n(x,s_j) = \frac{\Sigma_i N_i(x,s_j)}{\Sigma_i \int N_i(x,s_j)\mathrm{d}x}$$

- Intermittency Function

$$\Gamma_w(x) = \frac{n(x,\bar{s}(x))}{\max(n)}$$

- Comparison of Intermittency Function obtained by wavelet based method and hotwire method

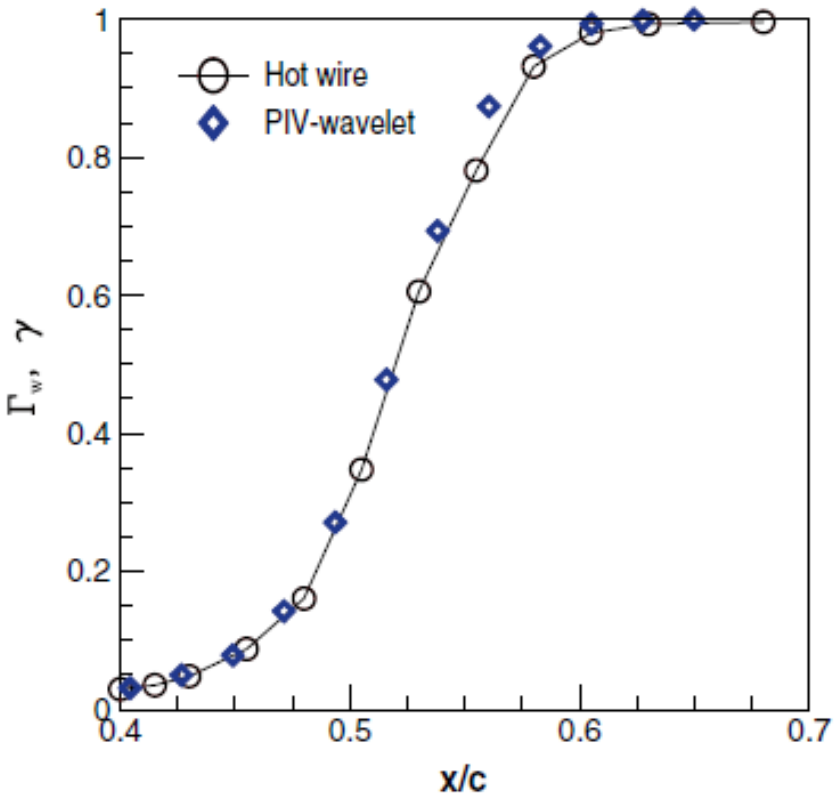

Comparison of intermittency obtained by hot wire measurements and wavelet technique, Simoni et al (2016)

Wavelet-based intermittency detection technique applied to present data

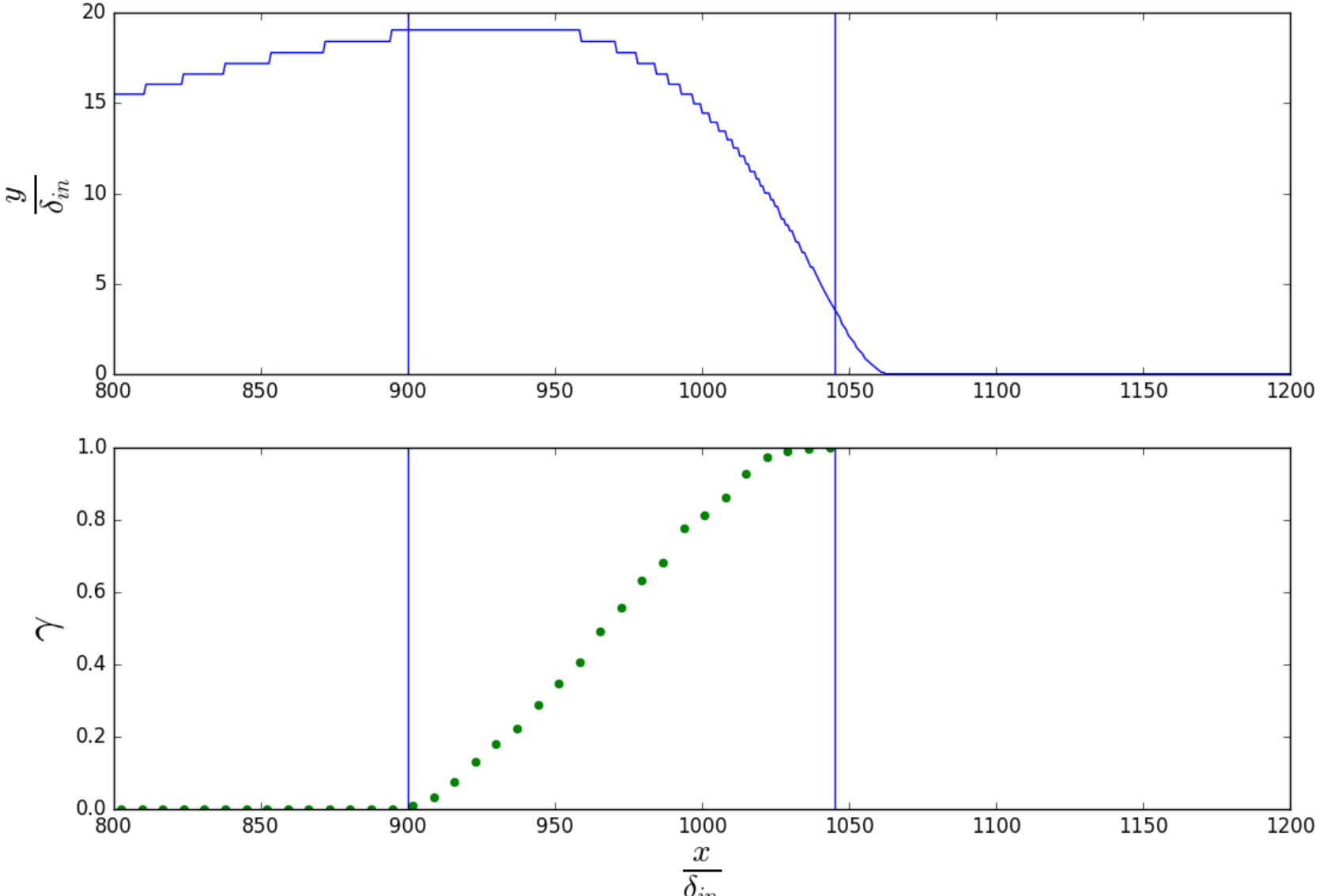

Effect of FST on Transition Location